In situ monitoring of the crack path in a Ti/SiC metal matrix composite

P. Lopez-Crespo[1a], A. Kyrieleis[1b], F. A. Garcia-Pastor[1c], M. Peel[2] and P. J. Withers[1d]

[1] School of Materials, Grosvenor St, University of Manchester, Manchester M1 7HS, UK
[a] pablo.lopezcrespo@manchester.ac.uk
[b] albrecht.kyrieleis@manchester.ac.uk
[c] francisco.garcia-pastor@postgrad.manchester.ac.uk
[d] philip.withers@manchester.ac.uk
[2] ESRF, 6 rue J Horowitz, 38000 Grenoble, France. matthew.peel@esrf.fr

ABSTRACT. *Synchrotron X-ray micro-tomography has been used to study the propagation of a fatigue crack in a Ti/SiC fibre composite of the type commonly employed in aeroengines. The experiments were conducted at the European Synchrotron Radiation Facility (ESRF) in Grenoble, France. The tomography data allowed us to follow the 3D crack path within the material and to analyse its interaction with the fibres non destructively. The tortuosity of the crack and the tilting of the crack front could effectively be evaluated with increasing number of cycles. Moreover the crack driving force was monitored in terms of crack opening displacement (COD) measured directly from the volume data.*

INTRODUCTION

The high specific strength and stiffness at elevated temperatures of titanium metal matrix composites (MMC) along with good elevated creep resistance make it an excellent material to be employed in different elements of aeroengines. As a consequence of the interaction between fibres and matrix, the fatigue behaviour of cracks in MMC tends to be even more complex than in unreinforced materials. Fibre crack bridging is often a dominant mechanism that substantially improves the fatigue resistance. A key parameter often employed for modelling crack bridging is the crack opening displacement, COD [1]. COD measurements are normally conducted on the surface. If the surface mechanisms are representative of the overall behaviour of the material, then microscopy techniques can be employed for characterising the fatigue behaviour of the material [2]. However, when the behaviour in the interior varies significantly, a thorough knowledge of the bulk evolution is advantageous. In addition, effects such as crack deflection and debris trapping within the crack are commonly

encountered in such systems. In order to build models capable of describing the behaviour of MMC under fatigue conditions, accurate characterisation of the crack path is required. This work presents a comprehensive 3D study of crack growth in a MMC. Powerful X-ray micro-tomography was employed for this purpose.

EXPERIMENTAL METHODS

The composite material used in this study was SCS6–SiC/Ti–6Al–4V, containing 35 vol.% of unidirectional fibres of 140μm diameter. The general distribution of the fibres within the matrix is shown in Fig. 1. A single edge cracked tension specimen with gauge section of $2.48 \times 1.08\,\mathrm{mm}^2$ was produced by EDM. Pure mode I load was nominally applied, oriented with the fibres perpendicular to the loading direction. The crack was grown in 7 steps. A summary of the different fatigue steps, number of cycles applied, average crack length, applied load and applied stress intensity factor, K_{nom}, are provided in Table 1. The nominal load ratio was approximately 0.1 throughout the experiment. No increase in the crack growth rate was observed with increasing number of cycles.

Table 1. Summary of fatigue crack parameters for each fatigue step.

Fatigue step	Fatigue cycles	Crack length, μm	ΔP, N	K_{nom}, MPa√m
FS0	96088	438	N/A	18
FS1	126088	664	1173	31
FS2	156088	891	1060	40
FS3	171088	968	980	42
FS4	186088	1062	825	41
FS5	201088	1099	815	43
FS6	241088	1214	879	57
FS7	281088	1430	975	93

The experiment was carried out on station ID15a at the European Synchrotron Radiation Facility (ESRF), Grenoble, France. X-ray micro-tomography in white beam mode was employed to image the crack. The pixel size was 1.58 μm. The application of this technique in a similar experiment is described in [3].

For convenience, the direction of crack propagation was taken as X-direction, the specimen thickness direction was taken as Y-direction and the longitudinal fibre direction as Z-direction. This is shown in Fig. 1.a.

CRACK EVOLUTION

The extension of the crack throughout the experiment was studied by extracting the minimum grey level along the Z-direction for each point (X, Y) of the volume

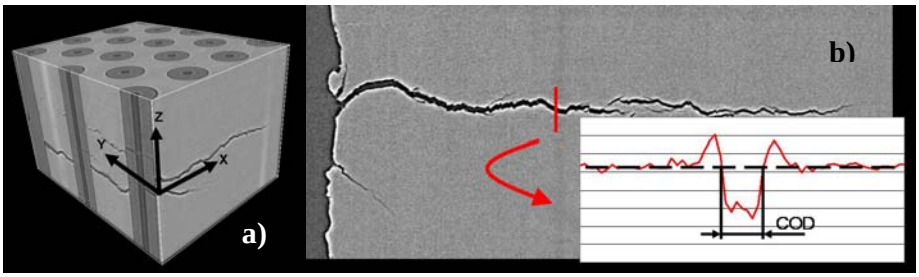

Fig. 1. a) General 3D view of a portion of the composite, where the fibre diameter is 140 μm and b) XZ view of the crack showing how the point-wise manual COD measurements are made.

reconstructed by micro-tomography. The cracked area in both matrix and fibres is shown as the dark regions in Fig. 2. It can be seen that a fibre close to the top left corner was already broken in the first stage FS0 (Fig. 2.a). In addition, a number of other fibres close to the crack mouth (left edge in Figs. 2) are thought to be damaged during the machining of the sample. The fact that one fibre was already broken, together with the likely damage of the fibres close to the top edge in Fig. 2, motivated a faster crack growth along one side. This resulted in the crack front tilting as the number of fatigue cycles increased. The crack length shown in Table 1 for each fatigue step was evaluated as the average between the crack length on either sides of the specimen.

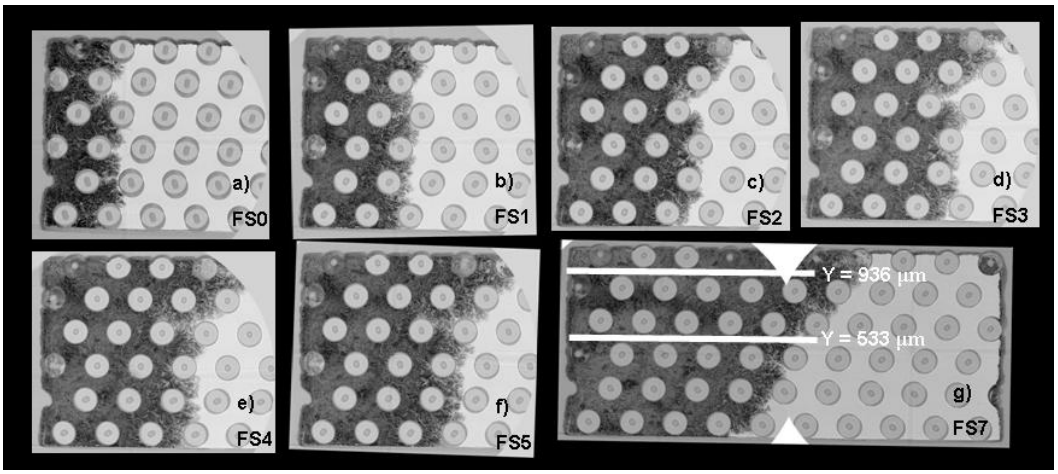

Fig. 2. Extension of the crack in successive fatigue steps at maximum load, showing the cracked area in dark. The crack advances from left to right. The diameter of the fibres is 140 μm.

In addition the tilting of the crack front was also assessed. Results for the seven fatigue steps are shown in Fig. 3. It can be seen that the crack front angle was approximately 0º for the initial stage (FS0). Then, because of the stress concentration

due to the broken fibres on one side (see Fig. 2), the crack front angle increases gradually, until a maximum of 32º. Perhaps surprisingly, the crack front progresses from a situation where only 3 fibres are simultaneously exposed to the growing fatigue crack, to a much more resistant layout (FS7), where 6 fibres are simultaneously exposed. For this last stage, 14 plies bridged the crack on one side and 8 plies on the other side of the specimen.

Tomography sections marked in Fig. 2.g at Y = 936 and 533 μm are shown in Fig. 4. The evolution of the crack at these particular positions can be appreciated in great detail. It is clear that the overall crack opening displacement (COD) increases as the crack grows with increasing fatigue cycles. This is confirmed quantitatively in Figs. 5 and 6. The amount of debris that can be found inside the crack increases as the crack grows. At X= 950 μm a large debris particle is evident in Fig. 4b. The crack morphology in previous steps (e.g. FS4) suggests that it may have been caused by the breaking off of the tip formed by the merging of two (connected) cracks running at different heights created as the crack went either side around a fibre. The wear of such particles can also be observed by looking at the size of the debris particle located at position X = 500 μm. As a consequence of the wearing between the crack face asperities and the debris, such particles become noticeably smaller and more rounded as the number of cycles increases.

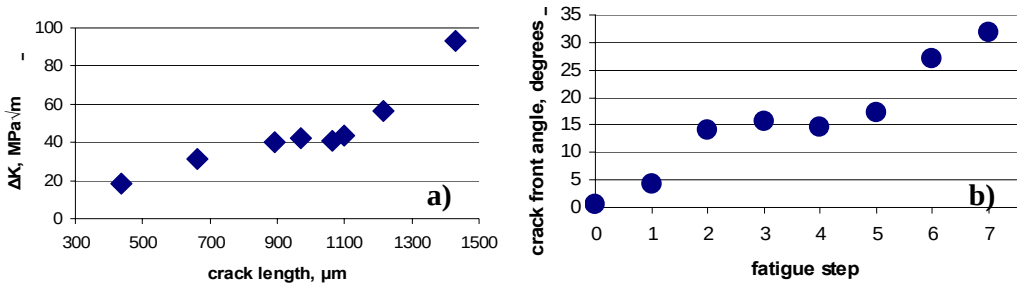

Fig. 3. a) Evolution of the crack front angle as the number of applied cycles (fatigue steps) increases. A crack front angle of 0º represents a crack front along Y. b) Nominally applied stress intensity factor versus crack length.

The discontinuity introduced as it by-passes the fibres often forces the crack to run simultaneously at different heights [3]. As a consequence, the tortuosity of the crack increases in the regions where two cracks meet. In addition, these regions are prone to have debris particles inside the crack. This effect can be observed for coordinates X = 175 μm in Fig. 4b. In contrast there are two cracks in FS0 that do not meet. Only subsequently (after FS2) do the two cracks meet. Finally in FS7, a debris particle appears at the location where the two cracks previously met.

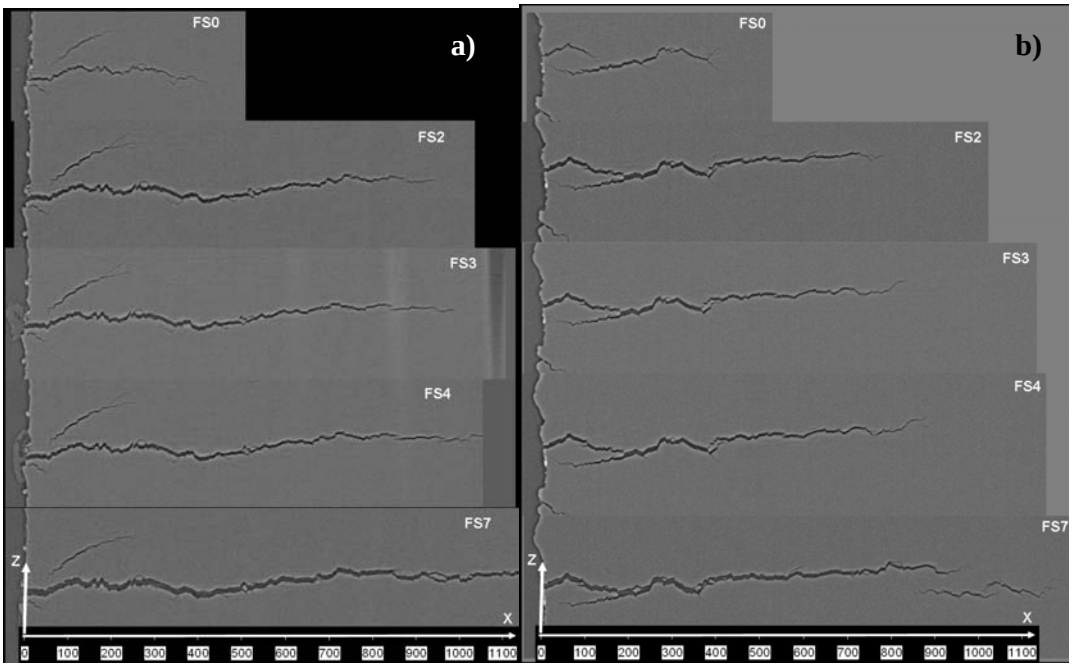

Fig. 4. Sideview cross-sections obtained by micro-tomography across the XZ plane for a) Y = 936 μm and b) Y = 533 μm. X-axis scale bar marked in μm.

CRACK OPENING DISPLACEMENTS

The accurate measurement of the COD across the thickness direction (Y) and along the direction of crack growth (X) could also be obtained by tomography. First, the crack profile has been extracted from the reconstructed volume by segmentation using VGStudio. To this end several points (seeds) were chosen within the crack volume. Using a region growing algorithm started from each seed, the crack volume was extracted. The reconstructed volume was then saved as a binary volume, i.e. with zero grey value everywhere except for the crack volume. The COD was measured by counting the non-zero voxels along the Z-direction. In this way, if more than one crack was found along the Z-direction (e.g. for X = 150 μm in Fig. 4) then the COD recorded is the sum of the opening of both cracks. Accordingly this COD measurement is referred to as the multiple-crack-COD, COD_{multi}.

The maps of COD_{multi} at 4 different fatigue steps are shown in Fig. 5. It can be appreciated that when the crack by-passes a fibre, a small matrix region ahead of the fibre remains un-cracked [3]. For some fibres, this effect persists even when the crack front has reached the following ply. The fibre located at (425, 250) is a good example. A matrix region of approximately 80 μm width still bridges the crack in FS2. Subsequently, in FS3, even though the crack front has already by-passed the next ply, there is a small corridor (coordinates (500, 250) in Fig. 5 FS3) of un-cracked matrix

connecting the fibre with the un-cracked ligament of the sample. After more than 100,000 cycles (FS7), the crack fully surrounds the fibre (Fig. 5).

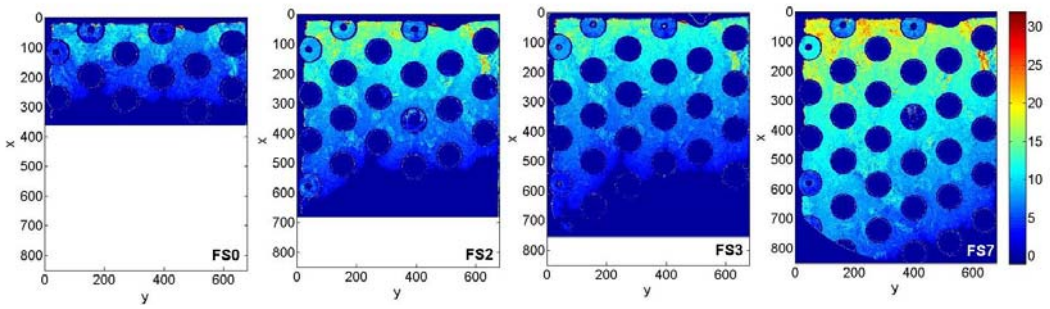

Fig. 5. Evolution of the total multiple-crack-COD, COD_{multi} mapped for 4 different fatigue steps with the composite dimensions expressed in voxel numbers and the COD expressed in microns.

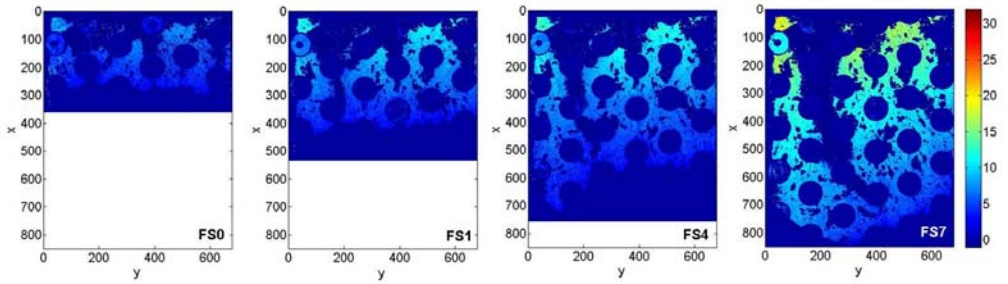

Fig. 6. Evolution of the COD (in μm) measured at 4 different fatigue steps. In this case, when more than one crack is found in the vertical Z-direction, then a COD value of -1 (dark blue) is given.

By contrast, Fig. 6 is obtained by considering the COD of only one crack. It can be seen that there is a region close to the top left corner where more than 1 crack exists. This effect extends as the crack propagates. As the crack by-passes unbroken fibres, the two fronts tend to propagate at different heights. This can be also observed from the side view in Fig. 4.b (X = 175 μm). While the two cracks do not connect initially in FS0, they do in subsequent fatigue steps. If the vertical distance between the two cracks is small, then there is a high chance that the two cracks will connect as the crack propagates. Because the two cracks were originally at different heights, the connection of the two cracks produces a step which together with other similar features makes the crack surface rougher. If on the other hand the distance is large enough, the connection between the cracks does not occur until further along the crack when the gap has become smaller.

The methodology was also adapted to measure the vertical coordinate (Z) of the crack as well as the number of cracks that exist at any location along the vertical Z-

direction. This is shown for the last fatigue step in Fig. 7. When more than one crack is found, a value of Z = 0 (dark blue) is given. First, one can see that mostly the crack has split into two cracks; only very rarely more than two cracks are seen. Fig. 7.a allows one to relate the size of the 2-crack-region after a fibre with the difference in heights of the two cracks. The 2-crack-regions below the fibres at (270,300) and (200,400) are relatively small (about 100 µm) and the heights of the cracks on both sides of the region are very similar. However, the 2-crack-regions below the fibre at (180,500) extends in X direction by about 150 µm, as observed also in Fig. 6. Fig. 7.a shows that the two cracks differ in height by 60-100 µm. Let us finally focus on the crack surrounding the fibre at (200,150) in Fig. 6, FS0. The following fatigue steps show that the 2 cracks do not manage to meet before FS7. The huge 2-crack-region extends from the initial fibre in by about 700 µm in X-direction and by-passing 5 plies. In this case, the difference of the crack heights to the left and to the right of that region is up to 140 µm. Hence the difference in vertical position of the crack in both sides of the fibres can be used to predict the size of the region where 2 cracks will propagate simultaneously.

The COD maps (Figs. 5 and 6) allowed the extraction of COD profiles along the crack growth direction at any position Y in the interior of the specimen as shown in Fig. 8. In addition, tomography allows the measurement of the COD in the XZ section views at any point. This is done by extracting a profile of the grey levels across the crack (Fig. 1.b).

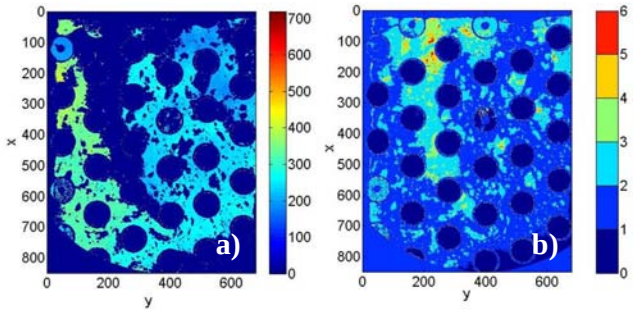

Fig. 7. a) Vertical coordinate (Z) in µm of the crack across the whole cracked area, b) Map showing the number of cracks stacked above one another at any X, Y location.

The crack tip location can be estimated automatically by considering the position where the COD curve equals zero. It can be also appreciated that the average slope of the COD is steeper for shorter crack lengths. This is probably due to the low number of plies bridging the crack for short cracks. The behaviour for short cracks, where only 1 or 2 plies bridged, more closely approximates to that for the unreinforced material. In these cases the change in COD between the crack mouth and the crack tip is more pronounced than for longer cracks, where a large number of plies are bridged. In such case the effect of a larger amount of fibres holding the crack shut gives rise to a flatter COD curve. Hence no increment is observed in COD at a fixed distance from the crack tip despite the much higher nominally applied K (Table 1).

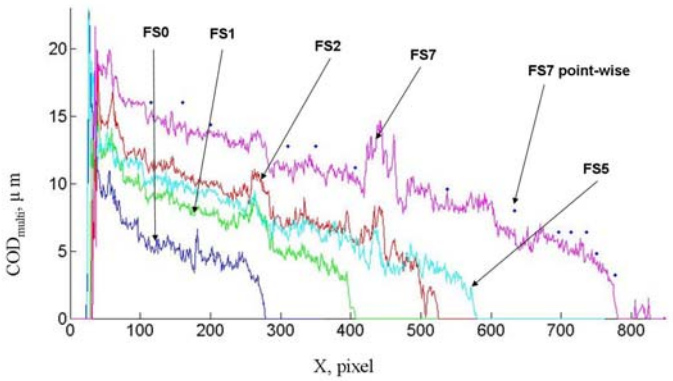

Fig. 8. Plot of COD versus crack length (X) for five different fatigue steps at Y = 452 pixels in the maps of Fig. 5. For FS7, the COD results obtained by manually measuring the COD are also included.

CONCLUSIONS

High energy synchrotron radiation was employed for monitoring the crack path within a MMC while fatigue load was applied. This was done by analysing 7 fatigue steps where up to 14 plies bridged the crack. A number of techniques were employed for determining the crack length, crack tip driving force (COD), height of the crack at any point as well as the number of cracks stacked above one another as any point. Despite the markedly increased ΔK applied as the crack grows longer, the rate of growth and the COD does not increase. Moreover the methodology enabled us to explore a number of features occurring in the interior of the specimen with high resolution. Possible mechanisms for the creation of debris particles trapped within the crack and other roughness effects are also proposed.

ACKNOWLEDGEMENTS

We are grateful to Marco Di Michel at the ID15 beamline for help with this experiment.

REFERENCES

1. K. S. Chan, *Acta Metall. Mater.* **41**, 761 (1993).
2. J. Liu, P. Bowen, *Metall. Mater. Trans. A* **34A** (2003).
3. Y.-C. Hung *et al.*, *Acta Materialia* **57**, 590 (2009).